International Journal of Applied Electromagnetics in Materials 2 (1991) 253–263
Elsevier

ELECTROMAGNETIC FIELD MODELING FOR NONDESTRUCTIVE TESTING OF COMPOSITE MATERIALS*,**

Nathan IDA
Department of Electrical Engineering, The University of Akron, Akron, OH 44325-3904, USA

Received 3 July 1991

The use of electromagnetic fields for testing of composites takes a variety of forms but most methods use high frequency techniques because of the properties of composites. Scattering and propagation in composites are good indicators of a variety of material properties, especially in low conductivity composites. Eddy currents at high frequencies can also be used for conducting composites. Some of the methods applicable to modeling of testing phenomena at high frequencies are reviewed here. Examples from testing of composites and dielectrics in microwave cavities and scattering from lossy dielectrics are given.

Introduction

The need to model high frequency nondestructive testing phenomena in dielectrics and in composite materials has led to investigation of a variety of methods suitable for this purpose. Most field computation methods neglect displacement currents, therefore are not suitable for computation at high frequencies. However, the neglection of displacement currents in eddy current formulations is not actually required for correct solution, nor does it provide a very significant advantage. The introduction of displacement currents in eddy current formulation is simple [1] and requires little change in formulations. This type of formulation allows the extension of eddy current methods to any frequency regardless of the significance of the eddy currents. Characterization of materials in microwave cavities can be most conveniently handled by solving the Helmholtz equation. While previous methods were plagued by spurious modes [10], the use of edge elements eliminates this problem completely. The formulation shown here is typical of the type of methods one can use for calculation of modes and their behavior as a function of material properties. A third method that is commonly used for high frequency calculations is the finite difference time domain (FDTD) method [6]. The use of finite differences is particularly useful for transient solutions but can be used equally well for time harmonic fields. The method incorporates radiation boundary conditions to allow modeling of scattering aspects. The use of radiation boundary conditions avoids reflections from artificial boundaries that would otherwise exist while still allowing modeling of all aspects of testing.

The use of these three methods, their formulation, and their use for characterization of materials at high frequencies is shown.

*Presented at the Third International Symposium on the Application of Electromagnetic Forces, Sendai, Japan, January 28–30, 1991.

**Supported in part by the National Science Foundation under grant EET8714628, and in part by The Ohio Board of Regents Academic Challenge Program. Computation facilities on the Cray Y-MP were provided by the Ohio Supercomputer Center.

2. Eddy current formulations

Eddy current formulations, normally neglect displacement currents and, therefore, cannot account for any of the propagation effects in materials. However, neglection of the displacement currents is more a convenience than a necessity. Eddy current formulations can be modified to allow computation of electromagnetic fields at high frequencies (such as in resonant cavities) by adding the coupling between the electric and magnetic fields. The effect of displacement currents can be added by including the electric field directly in the formulation, with little change in either implementation or computation. A general formulation, based on the magnetic vector potential and the electric scalar potential can be written as [1]:

$$-\nabla^2 \boldsymbol{A} = \mu \boldsymbol{J}_s + \omega^2 \mu \varepsilon \boldsymbol{A} - \sigma\mu(\mathrm{j}\omega \boldsymbol{A} + \nabla V)\,, \tag{1a}$$

$$\nabla \cdot (\mathrm{j}\sigma\omega \boldsymbol{A} + \sigma \nabla V) = 0 \tag{1b}$$

In equation (1a) the displacement currents were added in the term $\omega^2 \mu \varepsilon \boldsymbol{A}$. Equation (1b) is used to constrain the eddy currents in the solution domain using the continuity equation. Lorentz's gauge ($\nabla \cdot \boldsymbol{A} = -\mathrm{j}\omega\mu\varepsilon V$) is assumed in obtaining these equations.

Using the standard shape functions N for a finite element, the weighted residual integral over the element is written as:

$$\int_v \left(\frac{1}{\mu} (\nabla \times \boldsymbol{W}) \cdot (\nabla \times \boldsymbol{A}) + \frac{1}{\mu} (\nabla \cdot \boldsymbol{W})(\nabla \cdot \boldsymbol{A}) + \mathrm{j}\omega\sigma \boldsymbol{W} \cdot \boldsymbol{A} - \omega^2 \varepsilon \boldsymbol{W} \cdot \boldsymbol{A} + \sigma \boldsymbol{W} \cdot \nabla V \right) \mathrm{d}v$$

$$\int \left(W \cdot \frac{1}{\mu} \nabla \times A \times n + (W \cdot n) \frac{1}{\mu} (\nabla \cdot A) \right) \mathrm{d}s = \int \boldsymbol{W} \cdot \boldsymbol{J}_s \, \mathrm{d}v \tag{2a}$$

$$\int (\mathrm{j}\omega\sigma \nabla \boldsymbol{W} \cdot \boldsymbol{A} + \sigma \nabla \boldsymbol{W} \cdot \nabla V) \, \mathrm{d}v + \int \boldsymbol{W}(-\mathrm{j}\omega\sigma \boldsymbol{A} - \sigma \nabla V) \cdot \boldsymbol{n} \, \mathrm{d}s = 0\,,$$

where $\boldsymbol{W}$ are the weighting functions.

With N as the weighting functions and evaluating the various integrals, the discretized problem is written as

$$\begin{bmatrix} C + \mathrm{j}\omega\sigma D & \mathrm{j}\omega\sigma R \\ \mathrm{j}\omega\sigma U & \mathrm{j}\omega\sigma S \end{bmatrix} \begin{Bmatrix} \boldsymbol{A} \\ \dot{V} \end{Bmatrix} = \begin{Bmatrix} \boldsymbol{J}_s \\ 0 \end{Bmatrix} \qquad \dot{V} = \frac{V}{\mathrm{j}\omega}$$

where C and D are symmetric matrices and U, R, and S are row vectors.

A simpler formulation, one that neglects the scalar potential also exists [2] but inclusion of the scalar potential is more general. The constraint equation (i.e. $\nabla \cdot \boldsymbol{J}_e = 0$) is used to guarantee uniqueness in solution in conjunction with Lorentz's gauge. The solution of these equations leads to the correct field quantities based on the general field representation at any frequency. The magnetic flux density is calculated from $\nabla \times \boldsymbol{A}$ and the electric field intensity from $\boldsymbol{E} = -(\mathrm{j}\omega \boldsymbol{A} + \nabla V)$. While $\boldsymbol{B}$ and $\boldsymbol{E}$ are important quantities, for the purpose of detecting resonance or shift in resonant frequencies of cavities due to variations in material properties, it is more convenient to look at the total stored energy in the cavity. A peak in the stored energy indicates resonance. This choice is convenient in that the actual energy in the system is not important, only the relative values. Because of this, the source of the fields in the cavity is arbitrary as long as the modes the cavity can support are not altered by the source. Since modeling of the coupling into a cavity is quite complicated, this simplifies analysis considerably. In

addition, the Q-factor of a cavity can be calculated as:

$$Q = \omega \frac{W_s}{P_d + P_m}, \tag{4}$$

where W_s is the stored energy in the cavity, P_d are the dielectric losses and P_m are the conduction losses in the metallic walls of the cavity. These are given by:

$$W_s = \frac{1}{2} \int \varepsilon \boldsymbol{E} \cdot \boldsymbol{E}^* \, dv + \frac{1}{2} \int_v \mu \boldsymbol{H} \cdot \boldsymbol{H}^* \, dv, \tag{5}$$

$$P_d = \frac{1}{2} \int_v \sigma E \cdot E^* \, dv, \tag{6}$$

$$P_m = \frac{1}{2} \int R_s \boldsymbol{H} \cdot \boldsymbol{H}^* \, ds, \tag{7}$$

where R_s is the surface resistivity of the walls ($R_s = 1/\sigma\delta$), σ is the conductivity of the cavity walls and δ the skin depth. In geometries where the penetration might be deep, surface resistivity is not defined and P_m is calculated directly from $\boldsymbol{B}$ and $\boldsymbol{E}$. Conduction losses inside the cavity can also be accommodated in equation (4) by adding these losses to P_m or P_d. The integration of conduction losses inside the cavity is done over the volume in which they occur.

The use of this method allows calculation of resonant frequencies and quality factors but, the calculation of fields should be undertaken very carefully. The reason for this is that the source must be modeled (i.e. this is a deterministic rather than an eigenvalue problem). Unless the coupling to the cavity can be modeled accurately, the fields calculated are inaccurate. For the type of problems considered here both the resonant frequency and the Q factor can be taken as independent of the fields themselves. If the source is not modeled but, rather, assumed, the calculation of field values is irrelevant.

3. Characterization of materials in a microwave cavity

A second method of calculating fields at high frequencies is based on the solution of either of the following equations [3, 4]:

$$\nabla \times \frac{1}{\varepsilon_r} \nabla \times \boldsymbol{H} - k^2 \mu_r \boldsymbol{H} = 0, \quad \text{or} \tag{8}$$

$$\nabla \times \frac{1}{\mu_r} \nabla \times \boldsymbol{E} - k^2 \varepsilon_r \boldsymbol{E} = 0, \tag{9}$$

where $k = L\omega\sqrt{\mu_0 \varepsilon_0}$ and $\varepsilon = \varepsilon_r(1 + j\sigma\sqrt{\mu_0/\varepsilon_0}/(k\varepsilon_r))$ and L a spatial scaling factor. Time harmonic fields are assumed. A scaling factor is incorporated for convenience and its only effect is to reduce the magnitude of the constant k. This is later used for presentation of results but does not affect calculation. In equations (8) and (9), the relative permittivity and relative permeability are used. This is consistent with the way k is defined. The relative permittivity and permeability could be incorporated directly into k, removing them from equations (8) and (9).

Although not limited to NDT applications, our interest is in finding the resonant frequencies and the

corresponding field distributions in a microwave cavity containing a test specimen. Characterization of materials and material properties is then done using the shift in resonant frequencies and changes in the Q factor of the cavity. While not explicitly shown in this word the method works equally well for open resonant cavities. The cavity shape is arbitrary. The cavity wall is assumed to have finite conductivity and any materials within the cavity are characterized by $\{\mu_0\mu_r, \varepsilon_0(\varepsilon_r - j\varepsilon_r''), \sigma\}$. Spatial dependence for ε and σ is also implied for the purpose of this formulation. On material interfaces, $\boldsymbol{E}$ and $\boldsymbol{H}$ must be tangentially continuous. Boundary conditions are specified as $\boldsymbol{n} \times \boldsymbol{E} = 0$ on an electric wall or $\boldsymbol{n} \times \boldsymbol{H} = 0$ on a magnetic wall.

The weak form of equation (8) for the magnetic field is:

$$\int_v \left(\frac{1}{\varepsilon} \nabla \times H\right) \cdot (\nabla \times w_m)\, dv - k^2 \int_v \mu H \cdot w_m \, dV = -\frac{jk}{\eta_0} \int_s (n \times E) \cdot w_m \, dS$$

where $\boldsymbol{w}_m$ are any set of real, vector weighting functions. The use of vector or edge finite elements is chosen here to ensure elimination of nonphysical modes in the solution. For a tetrahedral element, the six edge shape functions and the finite element approximation are:

$$\boldsymbol{w}_n = \operatorname{sgn}(n) \frac{1_n}{\delta} (\boldsymbol{p}_{7-n,1} \times \boldsymbol{p}_{7-n,2} + \boldsymbol{e}_{7-n} \times \boldsymbol{r}),$$

$$\boldsymbol{H} = \sum_{n=1}^{M} H_n \boldsymbol{w}_n, \tag{12}$$

where H_n are the tangential components of $\boldsymbol{H}$ along edges. Edge elements guarantee that $\boldsymbol{H}$ is tangentially continuous on material interfaces. With vector weighting functions chosen to be the same as the shape functions, (eq. (11)), eq. (10) reduces to an eigenvalue problem. For the lossless case this reduces to the generalized algebraic eigenvalue problem:

$$[\boldsymbol{A}]\{\boldsymbol{H}\} = \boldsymbol{k}^2[\boldsymbol{B}]\{\boldsymbol{H}\}$$

For loaded cavities, (including lossy boundary walls), a complex eigenvalue problem must be solved

$$([\boldsymbol{A}] - \boldsymbol{k}^2[\boldsymbol{B}] + j\boldsymbol{k}[\boldsymbol{G}])\{\boldsymbol{H}\} = 0,$$

where the impedance boundary condition

$$\boldsymbol{E} \times \boldsymbol{n} = Z_m \boldsymbol{n} \times (\boldsymbol{n} \times \boldsymbol{H}) \tag{15}$$

was used to account for losses in the boundary walls. In this expression, Z_m is the surface impedance.

Similar forms may be written for frequency dependent dielectric loading [5].

The element matrices for the above two eigenvalue problems are:

$$a_{mn}^e = \int_{v^e} \left(\frac{1}{\varepsilon} \nabla \times w_n\right) \cdot (\nabla \times w_m)\, dv, \tag{16}$$

$$b_{mn}^e = \int_{v^e} \mu w_n \cdot w_m \, dv, \tag{17}$$

$$g^{e}_{mn} = -\frac{Z_m}{\eta_0}\int \boldsymbol{n}\times(\boldsymbol{n}\times \boldsymbol{w}_n)\cdot \boldsymbol{w}_m \,\mathrm{d}S$$

where η_0 is the intrinsic impedance in free space.

The discussion above (equations (10) through (18)) deals with the derivation in terms of the magnetic field. A similar derivation can be followed for the electric field, starting with equation (9) and its weak form:

$$\int\left(\frac{1}{\mu}\nabla\times \boldsymbol{E}\right)\cdot\left(\nabla\times w_m\right)\mathrm{d}v - k^2 \quad \varepsilon \boldsymbol{E}\cdot \boldsymbol{w}_m \,\mathrm{d}V = -\mathrm{j}k\eta_0\int(\boldsymbol{n}\times \boldsymbol{H})\cdot \boldsymbol{w}_m \,\mathrm{d}S$$

However, this will not be included here as the steps involved are sufficiently similar [5].

4. Finite difference time domain (FDTD) methods

A third method, well suited to calculations related to NDT is the finite difference time domain (FDTD) method. The main attraction of this method is in its ability to solve time dependent problems including transient applications. While the method can be easily used in three dimensional applications, we present here an axisymmetric formulation in terms of vector potentials as an example [6]. This has been found very useful in scattering problems, at microwave frequencies as well as for low frequency eddy current applications [7]. The equation to solve is:

$$\frac{\partial^2 A}{\partial z^2} + \frac{\partial^2 A}{\partial \rho^2} + \frac{1}{\rho}\frac{\partial A}{\partial \rho} - \frac{A}{\rho^2} = \mu\sigma\frac{\partial A}{\partial t} + \mu\sigma\frac{\partial^2 A}{\partial t^2}$$

To ensure a finite solution domain as well as to avoid reflections from artificial boundaries, radiation boundary conditions must be used. These boundary conditions are [6, 7]:

$$\frac{\partial A_0}{\partial r} + \mu_a\varepsilon_a\frac{\partial A_0}{\partial t} + \frac{1}{r}A_0 = 0 \qquad \text{in air}$$

and

$$\frac{\partial A_0}{\partial r} + \mu_m\varepsilon_m\frac{\partial A_0}{\partial t} + \left(\frac{\sigma_m}{2}\sqrt{\frac{\mu_m}{\epsilon_m}} + \frac{1}{r}\right)A_0 = 0 \qquad \text{in lossy dielectrics}$$

The more common condition $A_0 = 0$ is used for good conductors. In these boundary conditions, A_0 represents the outgoing component of A. Equivalent boundary conditions can be found for low frequency eddy current calculations and for time-harmonic fields [7]. Since eq. (20) does not include sources it is assumed that the effect of the sources is known through the distribution of A. This is normally found from independent calculations [6, 8].

As with any finite difference approximation, the discretization of space and time are linked by the Courant stability criterion (i.e. $(\Delta t/\Delta x)^2 < 0.5$). This imposes severe restrictions on the time steps that can be used, since the physical modeling of objects, often requires fine spatial discretization. The number of time steps is usually quite large.

The finite difference approximation uses explicit procedures with a central difference scheme to discretize the equations and a forward-backward difference scheme for the boundaries of the domain. Special treatment is also necessary for interfaces within the domain [7].

5. Results

The application of the eddy current formulation to the calculation of resonant modes in a cavity in the presence of a piece of lossy dielectric is shown first. A cubic cavity, 28.96 cm on the side is lined with alumina ($\varepsilon_r = 9$, $\sigma = 10^{-4}$ S/m), to create a cubic inner space, 20.32 cm on the side. A piece of carbon composite, ($5.334 \times 5.334 \times 4.826$ cm, $\varepsilon_r = 9$, $\sigma = 10^{4}$ S/m) is located at the bottom of the cavity. To obtain some some idea of the accuracy of results, the resonant frequency with a different cavity lining ($\varepsilon_r = 6$, $\sigma = 10^{-4}$ S/m) was measured. The measured resonant frequency for the empty cavity is 554 mHz, while the calculated resonant frequency is 564 mHz, or less than 2%. The results of the finite element calculation for the dimensions and properties shown above are shown in fig. 1, where the resonant frequencies with and without the composite are shown. As a reference, the resonant frequency for a dielectric test sample of the same size is also shown. Figure 2a shows some of the higher resonant modes for the same carbon composite. In comparison, fig. 2b shows the resonant mode at 1.922 GHz for the empty cavity. These calculations were done by scanning the required frequency range, solving the problem for each frequency and plotting the absolute value of the stored potential energy. Since the source has an arbitrary magnitude, the potential energy is shown as "normalized" and should only be viewed as a relative value. In these calculations energy is only used to detect resonance.

This method, while somewhat tedious in that scanning of a frequency range is necessary avoids the need for eigenvalue solution. It gives no information about the modes of the cavity. However, resonant frequencies are easily found while scanning can be done in selective ranges to minimize the number of runs. By starting at low enough frequencies, some of the resonant modes may be identified, especially in simple geometries from the modes of the empty cavity by assuming that the shift in resonant frequency occurs without changes in modes. In complexly loaded cavities this may not be possible. Minor peaks in stored energy between resonant modes are sometimes encountered (as in fig. 2) but these are normally very small compared to the resonant peaks that they do not interfere with

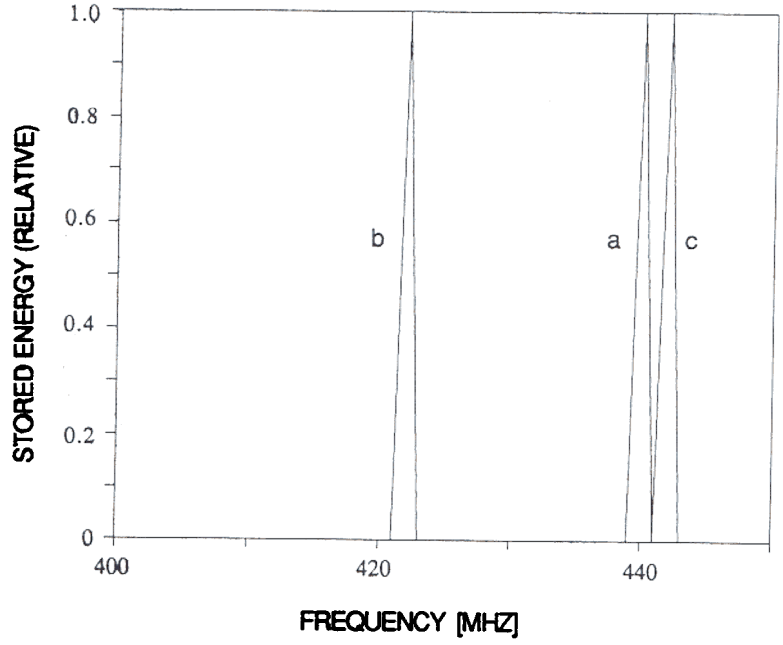

Fig. 1. First resonant mode in the cavity; (a) empty cavity, (b) with dielectric sample, (c) with carbon composite sample.

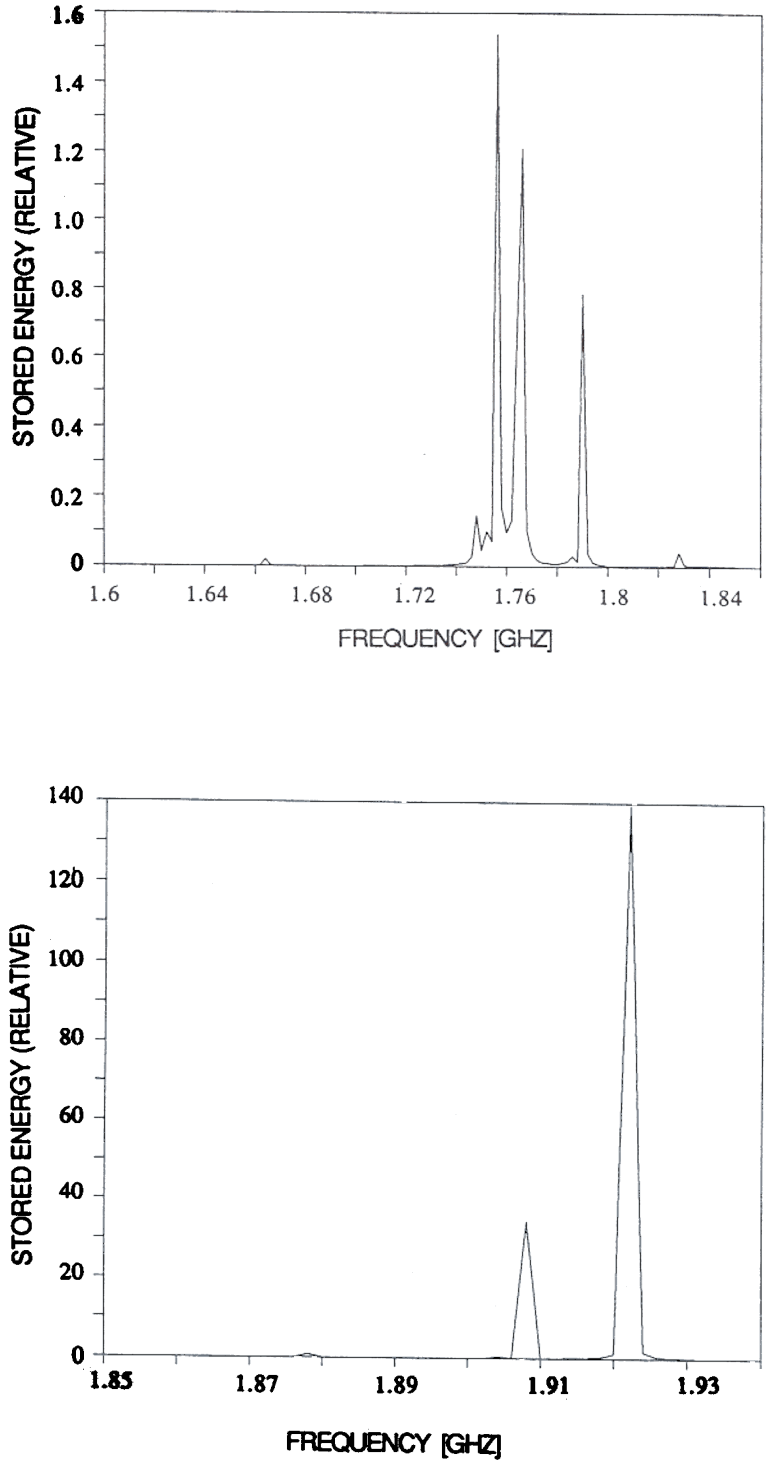

Fig. 2. Higher order odes; (a) resonant peaks at 1.756 GHz, 1.766 GHz and 1.790 GHz in the loaded cavity, (b) resonant peak at 1.922 GHz for the empty cavity.

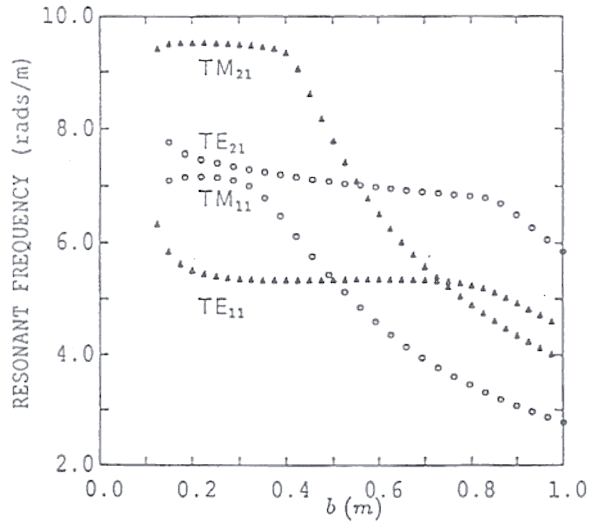

Fig. 3. Four modes of a dielectric sphere in a spherical cavity of radius b.

identification of resonance. While no specific effort was made to identify the minor peaks, they are probably due to mesh interfaces since their location on the frequency scale as well as their magnitude changes with mesh discretization. Mesh discretization need not be very fine for this type of problems since the resonant peaks are independent of mesh discretization. The size of the mesh is dictated by geometric considerations alone. The results shown in figs. 1 and 2 were obtained with 512 hexahedral (8 node) elements and 729 nodes for the whole cavity.

To demonstrate the use of the eigenvalue method for cavities, the first few modes in a spherical cavity, concentrically loaded with a spherical dielectric sample of radius 0.1 m are calculated. In this solution, the radius of the cavity is varied to obtain the mode curves. The first four modes were calculated for varying cavity radius b between 0.1 and 1 m. The results are shown in fig. 3 where the resonant frequency is given as k. The same problem can be calculated with a lossy sample, In fig. 4, the

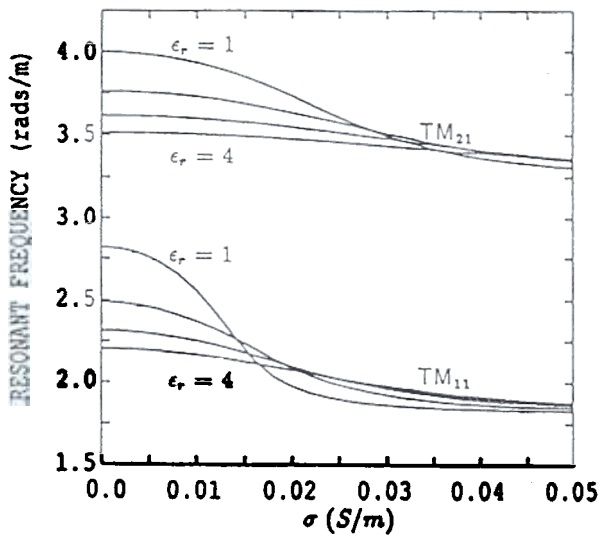

Fig. 4. Modes of a lossy sphere in a spherical cavity.

radius of the cavity is 0.5 m and the conductivity is varied. Results are shown for $\varepsilon_r = 1, 2, 3$ and 4 for TM_{21} and TM_{11} modes.

The method above was also used for other types of cavities and for materials with frequency dependent dielectric constants [5, 9]. While there are some difficulties in identifying the modes of the cavity, the method is general and useful in modeling loaded cavities. The use of edge elements also avoids the need to deal with spurious modes.

An example to the use of the FDTD method for NDT is the use of a small loop to generate a field in a dielectric or lossy dielectric. The scattered or transmitted field can be then used for analysis purposes. A small loop, with a diameter of 0.8 mm is used to generate a wave over a flat sample of a dielectric material. The field of the loop is calculated analytically [6, 8] and used as input to the FDTD program. Figure 5 shows the wave generated in a flat piece of dielectric ($\varepsilon_r = 6$, thickness of slab is 12.5 mm), as well as it's propagating properties. The small blank area is the loop area. Figure 6 shows the field in this region, clearly showing the "near field" pattern of the loop. Figure 7 shows propagation of the waves into sea water ($\epsilon_r = 80$, $\sigma = 4$ S/m) due to the same small loop located at the surface.

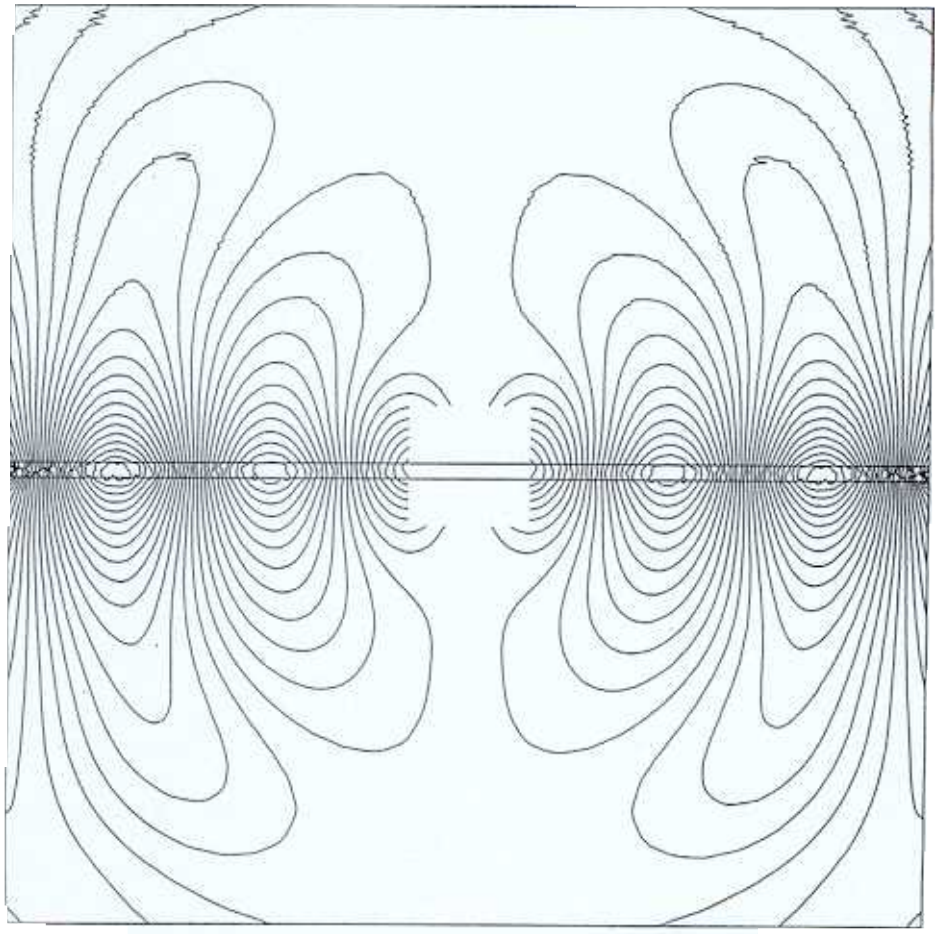

Fig. 5. Wave propagation in a dielectric slab due to a small loop

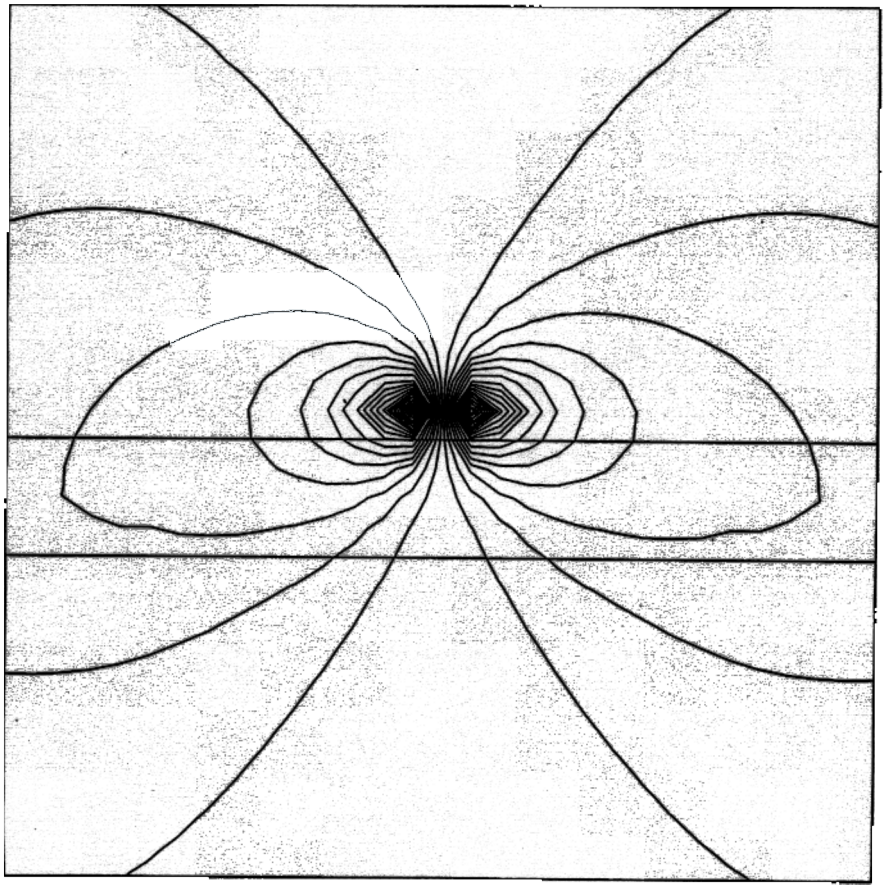

Fig. 6. The field of the loop in the "near field" region. This figure shows the field in the blank area of fig. 5.

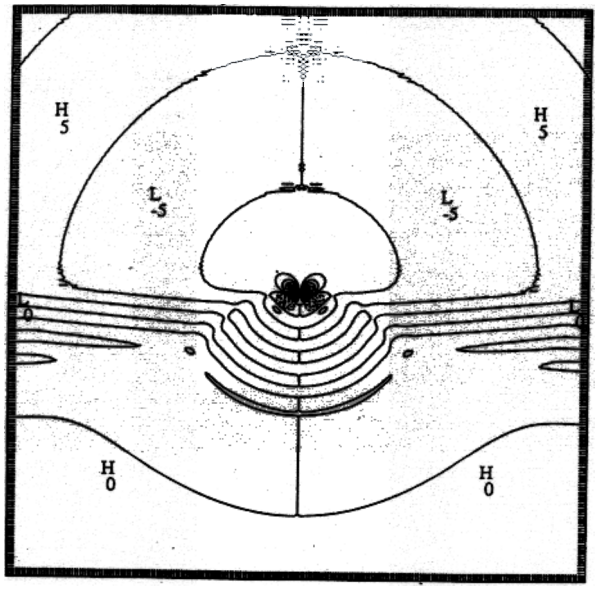

Fig. 7. Wave propagation in sea water due to a small loop at the surface.

A typical finite difference solution of this kind requires a mesh of the order of 100×100. As an example, the results obtained in fig. 5 were obtained with a 121×121 mesh resulting in a root mean square error throughout the solution domain of 4.75% compared to the analytic solution. This particular solution was obtained at 1 GHz, requiring a time step of 1.47×10^{-11} seconds. This yields a solution in 2700 steps, or after about 40 periods. While this is not a transient problem, it was solved as a transient problem for convenience and to demonstrate its flexibility. Although the number of points and the number of time steps are high, the solution itself is quick. The solution in figure 5 required about 2.3 minutes (on a SUN4/260). Solutions at lower frequencies are more complicated since they require considerably more time steps.

6. Conclusions

The three methods described here are only a sample of the formulations and variants one can use for computation of fields at high frequencies and their use for material characterization. The use of edge elements seems to be particularly important in computation in resonant cavities in order to avoid spurious solutions and simplify interpretation of results. The results shown are typical of the type of solutions one may need to find.

References

[1] H. Song and N. Ida, An eddy current constraint formulation for 3D electromagnetic field calculations, to appear in IEEE Transactions on Magnetics (1991).
[2] J.R. Brauer, R.H. Vander Heiden and A.B. Bruno, Finite element modeling of electromagnetic resonators and absorbers, J. of Appl. Phys. 63, No. 8 (April 15, 1988) 3197–3199.
[3] J.S. Wang and N. Ida, 3D finite element calculation of harmonic electromagnetic fields, IEEE Transactions on Magnetics 26, No. 2 (March 1990) 654–657.
[4] J.S. Wang and N. Ida, in: Review of Progress in Quantitative Nondestructive Evaluation, D.O. Thompson and D.E. Chimenti, Eds. (Plenum Press, New York, 1990) Vol. 9A, pp. 311–318.
[5] J.S. Wang and N. Ida, Eigenvalue analysis in electromagnetic cavities using divergence free finite elements, accepted for publication in: IEEE Transactions on Magnetics (1991).
[6] M.E. Lee and N. Ida, Axisymmetric electromagnetic fields coupled to lossy media, IEEE Transactions on Magnetics 26, No. 2 (March 1990) 575–578.
[7] M.E. Lee, S.I. Hariharan and N. Ida, Solving general time dependent two dimensional eddy current problems, J. of Computational Physics 89, No. 2 (August 1990) 319–348.
[8] J.R. Wait and K.P. Spies, Subsurface electromagnetic fields of a circular loop of current located above ground, IEEE Transactions on Antennas and Propagation, Vol. AP-20 (July 1972) 520–522.
[9] J.S. Wang and N. Ida, A numerical model for characterization of specimens in a microwave cavity, in: Review of Progress in Quantitative Nondestructive Evaluation, D.O. Thompson and D.E. Chimenti, Eds. (Plenum Press, New York, 1991).
[10] J.P. Webb, The finite-element method for finding modes of dielectric-loaded cavities, IEEE Transactions on Microwave Theory and Techniques, Vol. MTT-33, No. 7 (July 1985) 635–639.